Vol. 80 Commemorative Accounts

Theoretical Studies of Chemical Reactions—A Fascinating World of Chemistry from Gas-Phase Elementary Reactions through Nanostructure Formation and Homogeneous Catalysis to Reactions of Metalloenzymes

Keiji Morokuma

Fukui Institute for Fundamental Chemistry, Kyoto University, Kyoto 606-8103

Cherry L. Emerson Center for Scientific Computation and Department of Chemistry, Emory University, Atlanta, Georgia 30322, USA

Received July 26, 2007; E-mail: morokuma@fukui.kyoto-u.ac.jp

Theoretical/computational studies of chemical reactions provide insight into detailed pathways and energy profiles that are not easily available from experiments. Although finding the potential energy profile for ground-state reactions of small molecular systems has become routine, there are many challenges in theoretical studies of chemical reactions. There are still a lot to learn from gas-phase reactions of small molecular systems, starting from an excited state and cascading though many potential surfaces via conical intersections. Molecular dynamics using quantum mechanical energy (QM/MD) was found to be an ideal tool for study of reactions occurring far from equilibrium, such as formation of fullerenes from small carbon fragments and growth of carbon nanotubes. Challenges in theoretical studies of homogeneous catalysis are subtle ligand effects, involvement of multiple spin states and cooperative effects of multiple metal centers. Discussions here cover stories on activation of molecular nitrogen by zirconium complexes, olefin epoxidation by Salen complexes and reactions of tri-ruthenium complexes. Metalloenzymatic reactions have been discussed using protein models with ONIOM QM:MM approaches as well as active site models. Cases are presented where the enzymatic environment makes rather small effects, where it makes energetically significant effects and where it participates positively into the reaction coordinate.

1. Introduction

The chemical reaction, a central theme of chemistry, is usually a complicated sequence of bond-breaking and formation processes and takes place in gas phase, in solution, on surfaces and interfaces as well as in protein and other biological environments. Modern experimental studies give accurate measurements of rates, selectivity, branching ratios, mechanisms, and dynamics of chemical reactions. Theoretical studies of chemical reactions started soon after the quantum mechanics was discovered. Earlier theoretical studies were mostly limited to reactivities of π-electron systems using the Hückel method, but they nevertheless have led to major discoveries including symmetry rules in organic reactions. When the author started his graduate studies exactly fifty years ago, the only "computer" available for frontier density calculations was a hand-driven calculator (Fig. 1), which is estimated to be at least 10^{15} slower than the present supercomputer. Thanks to the development of high-accuracy theoretical methods and availability of high-speed computers, theoretical calculations nowadays can provide detailed and reliable information as to potential and free energy surfaces, transition states, reaction pathways as well as dynamics of chemical reactions; some of such information is very hard to obtain experimentally

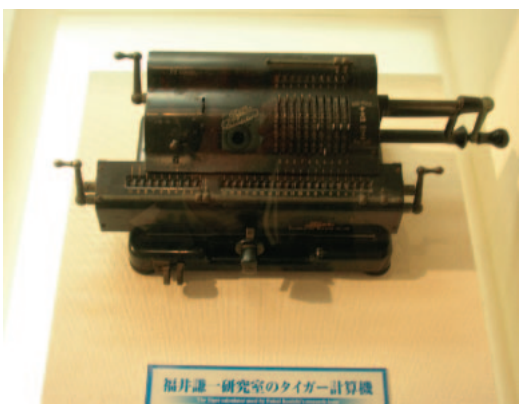

Fig. 1. Hand-driven calculator used in Kenichi Fukui's laboratory in 1950's, presently on display at the 100-Year Memorial Hall of Kyoto University.

Published on the web December 13, 2007; doi:10.1246/bcsj.80.2247

and is thus complimentary to experiments. However, theory often simplifies and approximates the complicated real reaction system and needs to be verified experimentally. Therefore, strong collaboration between theory and experiment is essential for understanding of chemical reactions.

The availability of user-friendly software and high-speed computers, as well as the advent of qualitatively reliable and yet computationally less demanding quantum chemical methods (such as density functional theory (DFT)), popularized theoretical studies of chemical reactions. Any experimentalist can buy such a software and a few PCs and calculate routinely with a reasonable accuracy structures and energies of reactants, transition states, intermediates, and products of chemical reactions in the ground state involving up to 50 or so atoms. In a sense, theory/computation became a tool available to everybody, as NMR, IR, and other measurements did. It is nowadays nearly impossible to find major experimental papers without theoretical/computational discussions. However, a word of warning may be in order concerning untrained and nondiscriminatory use of computational results. These convenient program packages can give wrong results, if inappropriate methods or approximations are used. It often requires expertise or extensive training to find out right from wrong and to analyze the results correctly. Collaboration with or at least advice from experts is strongly recommended, at least at early stages of theoretical studies performed by experimentalists.

Although many problems of chemical reactions have been solved or can be routinely answered by existing theoretical methods, there are also many challenges that need to be resolved by theoretical studies. One of such challenges are chemical reactions in excited states. Excited states are much harder to correctly describe quantum mechanically; for instance, popular density functional approaches had limited successes here. Excited-state reactions usually involve many electronic states and take place by cascading through these potential energy surfaces via conical intersections or seam of crossing between states of different spin states. Another grand challenge is reactions in complex systems, including reactions in solution, on surfaces and in biological environments. The main stream of chemistry has been moving toward development and design of more and more complex molecular systems. Such systems are often too large to be handled by conventional quantum chemical methods and have too many degrees of freedom to describe potential energy surfaces in a conventional manner. One has to utilize all available theoretical methods, not only quantum chemistry but also molecular dynamics and statistical mechanics, to address to these complex problems. "High-accuracy simulation of complex molecular systems" is one of the new challenges for theoretical chemistry.

The potential energy surface is the most basic information needed for theoretical studies of chemical reactions. Quantum chemists over the years developed a series of approximate theoretical methods to describe potential energy surfaces. High-level ab initio methods can accomplish chemical accuracy ($<1\,\mathrm{kcal\,mol^{-1}}$); however, their high-order dependency ($\approx N^6$) on the size of molecule prevents it to be used routinely for molecules with more than tens of non-hydrogen atom, despite recent advent of linear-dependent algorithms and parallelization. Density functional methods give mid-level ($\approx 5\,\mathrm{kcal\,mol^{-1}}$) accuracy at mid-level cost and size-dependency. Semiempirical methods are low cost alternatives with lower reliability. Classical molecular mechanics (MM) force field is very fast and can be applied to very large ($>10^6$ molecules) systems; however, its reliability is limited and cannot usually handle bond-breaking or formation. It is therefore impossible to simulate reactions of a complex molecular system (say 10^4 atoms) accurately for long periods of time (say 10^{-9} s) using a single level of method. In order to solve such a demanding problem, it is almost mandatory to adopt a combination of these methods or a hybrid method; for instance a highly accurate but costly method for the most important part (say where the reaction is taking place), a medium-accuracy medium-cost method for the immediate neighborhood and an even less accurate and less costly method for the environment. The most popular hybrid method is what is called QM/MM method, in which a quantum mechanical method (QM) is combined with the MM method.[1] The ONIOM method developed in our group allows combination of various levels of theory in multiple layers, including QM:MM, QM:QM, and QM:QM:MM.[2] Unfortunately whenever one combines QM and MM, there arises a nasty arbitrariness of scaling charges in the interface region, and we advocate the QM:QM:MM three-layer method as means of avoiding such complications.[2g]

With all the above background in mind, in the present article we will briefly review some of our own recent studies toward these challenges of theoretical studies of chemical reactions. This is still a fascinating world of chemistry.

2. Gas-Phase Excited-State Reactions—A Case of Photodissociation of Chlorine Azide (ClN_3) to Produce "Cyclic-N_3"

A photochemical reaction starts from an excited electronic state with large electronic energy. The potential energy surface of one electronic state with 3N-6 degrees of freedom can cross with other potential energy surfaces in 3N-8 degrees of freedom, and these crossings (called conical intersections) are the most likely places where the system makes transition from one electronic state to another. The reaction takes place by cascading through multiple excited states to reach multiple products. Experimentalists can use lasers to excite a molecule to many different excited states, almost as they wish, and observe different products, rate, dynamics of such reactions. However, it is very hard to interpret the experimental results solely based on chemists' commonsense that has been built mainly for ground-state reactions. In order to understand what is actually taking place during the photochemical reaction, it is almost indispensable to mobilize the help of theoretical computations. We have collaborated strongly for many years with experimentalists in photodissociation reactions as well as ion–molecule reactions, which usually start from the ground-state reactants of an ion and a neutral molecule but cascade through many potential energy surfaces to product a series of products in ground and excited states.[3] In the present article, we will show one recent example of our studies: photodissociation of ClN_3 at 157 nm to produce "cyclic" N_3.

The photodissociation of ClN_3 has been recently studied experimentally at a variety of excitation energies ranging from

115.3 to 181.6 kcal mol^{-1}.[4] One interest in these experiments is producing "cyclic"-N_3, i.e. the triangular N_3 isomer. The cyclic-N_3($^2B_1$), an isosceles triangle with the apex $\angle NNN = 49.8^\circ$ and the two equal N–N bond lengths of 1.4661 Å, lies about 30 kcal mol^{-1} above the linear $\tilde{X}^2\Pi_g$ ground state and is separated from the latter with a large barrier.[3b] Two dissociation pathways were observed, i.e. a molecular elimination producing NCl + N_2 and a radical bond rupture producing Cl + N_3. The radical bond rupture pathway is overwhelmingly preferred and produces a mixture of linear ground-state N_3 and a "high-energy form" (HEF)-N_3 attributed to the cyclic N_3. In the recent 157.4 nm experiment,[4c] HEF-N_3 was the exclusive N_3 photoproduct.

Our recent theoretical calculations (Kerkines, Wang, et al.)[5] showed that the 157 nm excitation brings the system to the seventh singlet excited state S_7 ($4^1A'$) of ClN_3. Dynamics of the molecule excited to S_7 at the Franck–Condon geometry ($t = 0$) was followed by a trajectory adopting a high-level ab initio method (sa(4)-CASSCF(14e/12o)/6-31G*). This excited molecule was found to dissociate to N_3 + Cl smoothly without going over a barrier. At the instance of dissociation ($t = 39.9$ fs), the produced N_3 has a bent geometry of $\angle NNN$ of 126° and NN distances of 1.27 and 1.37 Å and is in 2 $^2A''$ ($^2B_1$ in C_{2v} notation) or 2 $^2A'$ ($^2A_1$) excited electronic state of N_3, corresponding approximately to ■ mark in Fig. 2 (a cut of potential energy surfaces of N_3 as function of $\angle NNN$ assuming C_{2v} symmetry with two equal NN distances of 1.41 Å). The trajectory of N_3 starting at this geometry (removing Cl atom) on the 2 $^2A''$ ($^2B_1$) cannot isomerize to "cyclic" N_3 due to a high barrier at $\angle NNN \approx 85^\circ$. On the other hand, the N_3 trajectory on 2 $^2A'$ ($^2A_1$) found a conical intersection with 1 $^2A'$ ($^2B_2$) at $t = 44.4$ fs, corresponding approximately to the first ■ mark in Fig. 2. The non-adiabatic coupling between the two states is small, and the trajectory is likely to path through this cone (diabatically) and propagate on the same surface, now called 1 $^2A'$ ($^2A_1$). This trajectory was found to meet

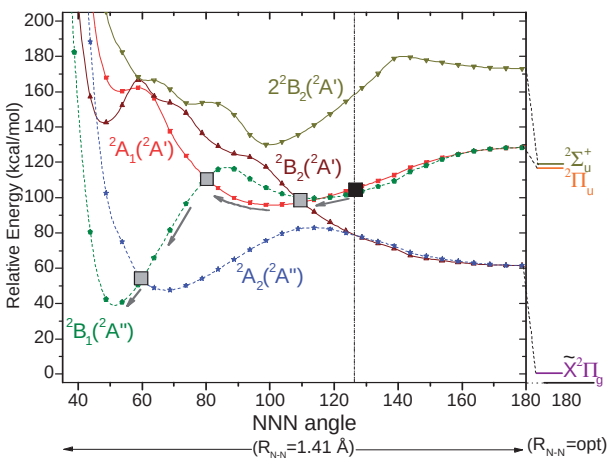

Fig. 2. Cut of potential energy surfaces of N_3 molecule, and qualitative pathway for formation of cyclic N_3 from bent excited N_3 formed by photodissociation dissociation of ClN_3 on the S_7 state, which dissociates to give an excited state of N_3 at a bent geometry (■) and traverses through various conical intersections (■) to produce cyclic N_3 ($^2B_1$).

another conical intersection with 2 $^2A''$ ($^2B_1$) at $t = 63.3$ fs, corresponding approximately to the second ■ in Fig. 2. Although the probability of making non-adiabatic transition from 2 $^2A'$ ($^2A_1$) to 2 $^2A''$ ($^2B_1$) is not large at each crossing, the trajectory continued on 2 $^2A'$ ($^2A_1$) vibrates repeatedly within its attractive potential well and crosses with 2 $^2A''$ ($^2B_1$) many times, giving this non-adiabatic transition non-negligible probability. The trajectories that made transition to 2 $^2A''$ ($^2B_1$) can lose internal energy and give "cyclic" N_3 species in the $^2B_1/^2A_2$ conical intersection region (the third ■) or some of them may dissociate to N (^1D) + N_2.

Although hard to confirm experimentally, this kind of proposed complex pathway provides insight into the mechanism of chemical reactions involving multiple potential surfaces. We feel that there are still many basic matters to learn from relatively simple molecular systems.

3. Formation and Growth of Carbon Nanostructures

3.1 "Shrinking Hot Giant Fullerene Road" of Fullerene Formation. Despite all the activities concerning fullerenes, the mechanism of formation of fullerenes from small carbon clusters is not known.[6] Many hypothetical models have been proposed, including "nautilus model," "pentagon road," "fullerene road," "ring-stacking," and "ring fusion spiral zipper" mechanism, but none of them has any solid foundation.[7] Moreover, these mechanisms rely on a principle by which the highly symmetric fullerene cage is built from smaller units in a systematic, step-wise way. The violent conditions of fullerene formation make such an organized approach very implausible.

Traditional quantum chemical approaches to find transition states and intermediates through growth pathways have been attempted, but one recognizes immediately that there are too many possible pathways. Hot carbon vapor is a system far from thermodynamic equilibrium, and such systems may give rise to auto-catalysis and self-assembly processes associated with irreversible processes.[8] Therefore, molecular dynamics (MD) approach has to be used in which many pathways are explored by trajectories, and trajectories have to be run a long time (>100 ps).

In long time MD, inexpensive MM potential is typically adopted. MM, which usually cannot describe bond-breaking and formation process, can be modified to treat bond-breaking and formation and has been used for carbon cluster simulations.[9] However, the reactivity of sp^2-carbon is controlled by π-conjugation, as known from the Hückel age, and this necessitates quantum mechanics (QM). It turned out that DFT, a typical QM method, is about 10^6 more expensive than MM and cannot be used for simulation of >100 ps. We found that the density functional tight-binding (DFTB) method,[10] an approximate or semiempirical quantum mechanical method, is 10^{2-3} times faster than the DFT method, properly treats π-electrons, gives reasonable qualitative reliability, and still is fast enough for dynamics. It should be noted that there have been some simulations of fullerene and carbon nanostructure formation using the reactive MM, and nanosecond or longer has been proposed as the time scale for the self-assembly.[11]

We (Irle, Zheng, Wang, et al.)[12] have performed extensive QM/MD simulation of the formation of fullerenes from small

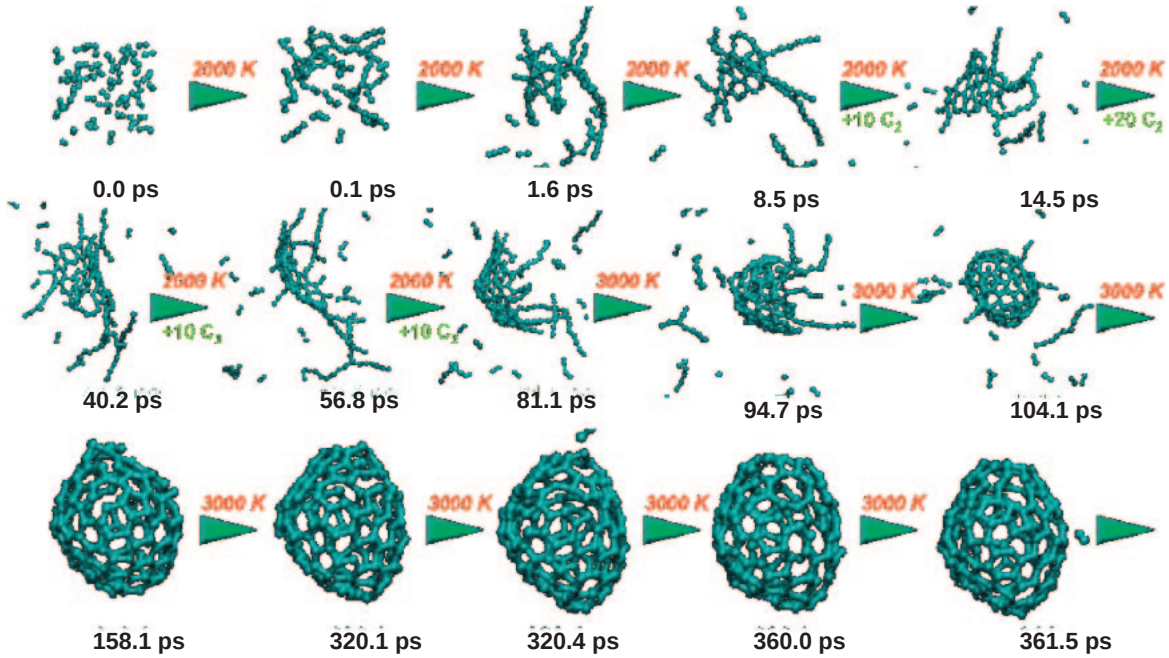

Fig. 3. "Shrinking Hot Giant Fullerene" mechanism of fullerene formation from small carbon fragments. The self-assembly (size-up) process (up to 104.1 ps in this example) took place through different stages: nucleation of polycyclic structures from entangled polyyne chains, 2. repeated growth via "octopus-on-the-rock" structures, consisting of the familiar ring condensation of carbon chains and rings attached to the hexagon and pentagon containing nucleus as well as the chain-growth by addition of more C_2 fragments to the peripherals, and finally 3. cage closure where polyyne chains reach over the opening and "zip" them closed. Only giant fullerenes are formed. The size-down or shrinking process shed the antennae chains quickly and then very slowly loses C_2 fragments from giant fullerenes by "pop-out" events (seen at 320.4 ps) to produce smaller fullerenes (Adapted from Irle et al., Ref. 12g. Reprinted with permission. Copyright 2006 World Scientific Publishing Company).

carbon fragments. Based on the results, we have proposed a new mechanism of fullerene formation, called "Shrinking Hot Giant" road, as illustrated in Fig. 3.[12e] We were able to "make" fullerenes in QM/MD simulation when pretty high-concentration of small carbon fragments, for instance 60 C_2 molecules in 30 Å cubic box, are heated at 2000 to 3000 K and further supplied with additional 10 C_2 molecules several times every 6 ps. The addition serves only in the interest of computer resource reduction, we have later achieved the same result by supplying all C_2 molecules from the beginning.[12g] The entire self-assembly (size-up) process went through three different stages: 1. nucleation of polycyclic structures from entangled polyyne chains (irreversible carbon sp^2 re-hybridization from sp-hybridized polyynes), 2. repeated growth via "octopus-on-the-rock" structures, consisting of the familiar ring condensation of carbon chains and rings attached to the hexagon and pentagon containing nucleus as well as the chain-growth by addition of more C_2 fragments to the peripherals, and finally 3. cage closure where polyyne chains reach over the opening and "zip" them closed, which is likewise irreversible due to the gain of energy in eliminating all dangling bonds. We were able to make about 20 fullerene-like cage structures in approximately 5–25% of trajectories (depending on the carbon density; the rest producing irregular octopus-on-the-rock structures resembling more like graphenes and chains without cage), suggesting that the cage formation through this mechanism is not a rare event.

The "size-up" self-assembly process forming a cage from C_2 fragments is completed in 40–100 ps (104.1 ps in the example in Fig. 3), much faster than the MM/MD simulations suggested, because of high reactivity of unsaturated π-electron systems. Another interesting feature of the successful trajectories is that only "giant fullerenes" containing 100 to over 200 carbon atoms in the cage are formed, with chains ("antennae") of polyynes attached on the surface. We could not make any C_{60} or other smaller fullerenes found commonly in experiments. In order to form a cage structure, a curvature has to build up by creating five-membered rings at strategic points. Although many five-membered rings as well as six- and seven-membered rings are formed, a steep curvature needed for formation of smaller fullerenes is very hard to come by and a large number of carbon atoms are needed to gradually build curvature and close a cage.

Then, the next question is how smaller common fullerenes are formed. In order to see whether giant fullerenes formed above can become smaller, we continued heating the structures formed above and show an example in the second half of Fig. 3. The antenna chains were found to "fall off" quickly within a few tens of ps after the closure. Then, C_2 fragments were found to "pop out" from the vibrationally hot cage very slowly at an average rate of roughly one C_2 fragment for every few to several tens of ps. Prerequisite for the formation of a pop-out C_2 unit is violent motion concentrated in a specific part of giant fullerenes, and that these motions occasionally set "wobbling C_2" units free, leaving a radical center at the other end of the now opened cage that closes again quickly. As giant fullerenes shrink and become more and more spherical, such pop-out events occur less and less frequently, and

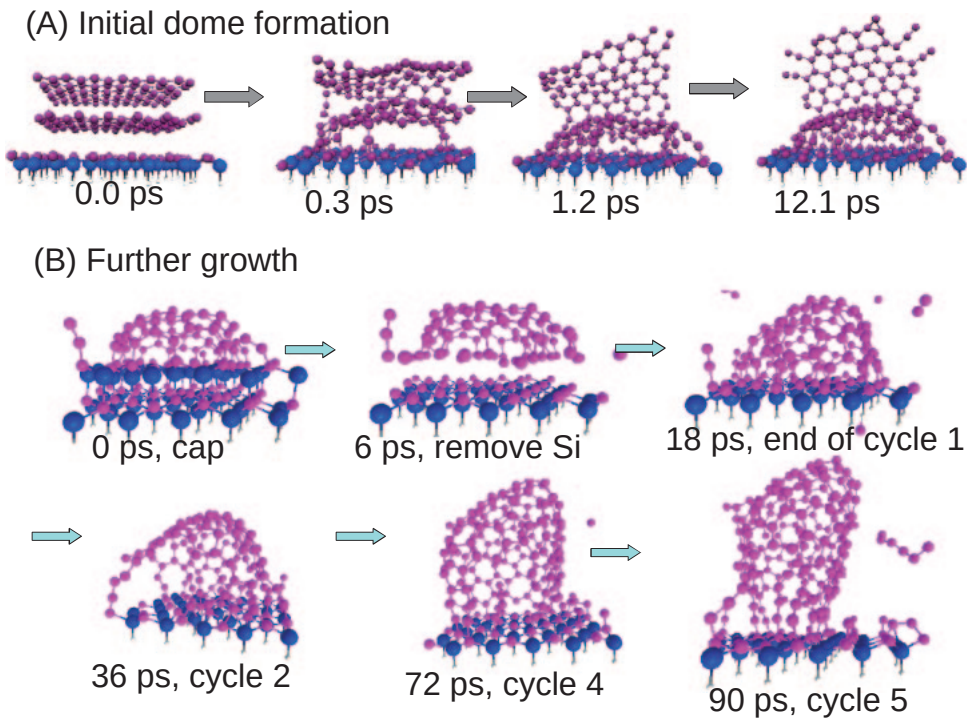

Fig. 4. (A) Initial formation of carbon dome on the C-face of surface of SiC. (B) Growth of carbon nanotube form the initial carbon dome. The top silicon layer was removed suddenly at 6 ps and very 18 ps thereafter (Adapted from Wang et al., Ref. 16b. Reprinted with permission. Copyright 2007 American Chemical Society.).

the shrinking is significantly slowed down. We proposed that this slow but long "size-down" process eventually results in thermal distribution of a variety of fullerenes.

This fullerene formation mechanism is a good example for dynamic self-assembly leading to dissipative structures far from thermodynamic equilibrium, and the "shrinking hot giant" road we proposed provides a natural explanation for the observed cage size distributions by way of a random optimization process consistent with several important experimental observations. Recently, we have been studying using DFTB/MD the mechanism of formation of metallofullerenes, fullerenes with metal atoms inside the cage.[13] Different metals show different behaviors. For instance, Sc atoms interacts with the forming open-cage fullerene structure weakly and prefers to stay in the vicinity of the mouth of the open-cage, and when the cage closes, it tends to be excluded from inside the cage. On the other hand, Ti atoms interacts with the inside of open cage and tend to be trapped more inside the cage when closed.

3.2 Mechanism of Growth of Carbon Nanotubes on SiC Surface during Thermal Decomposition. Carbon nanotubes are grown in most cases using a variety of techniques (such as arc discharge or laser vaporization of graphite as well as chemical vapor deposition) in the presence of transition metal catalysts.[14] In an exceptional case, carbon nanotube can be grown on the SiC surface by high-temperature thermal decomposition.[15] In this case, nobody knows how but everybody assumes that Si atoms depart the system leaving behind carbons to reorganize. The growth mechanism of carbon nanotubes has been a subject of active studies, but has not been well established.[15b]

We (Irle, Wang, Zheng, et al.)[16] used the DFTB-based QM/MD method here again to study the mechanism of carbon nanotube growth on the SiC surface. High-temperature simulations have been performed on model systems of "thin" SiC crystal surfaces with two graphene sheets placed on top of either C or Si face. In agreement with experiment, we find that, as shown in Fig. 4A, the C face-attached graphene layer warps readily to form small diameter, stable nanocaps, and anneals to dome-shape structures with zigzag chirality. On the other hand, the Si face-attached graphene sheet does not readily warp and forms more volatile Si–graphene bonds. Our explanations are as follows: 1. CNT caps only nucleate on the C-face due to the two antagonistic forces attempting to form a balance: formation of strong C–C bonds between top–layer graphene and dangling C surface valences on one hand, and the resistance of the planar sp^2 graphene sheet to take non-planar sp^3 hybridization. 2. Si atom removal leads to unstable carbon species with dangling bonds which make stable connections with existing carbon material on the surface, thereby continuing to grow existing caps into tubes. 3. Dangling C atoms on the Si-face are protected by the Si atoms as opposed to the C-face, and rather tend to form graphene layers among themselves.

In order to further simulate the growth of carbon nanotube, we used a slightly different model and continued heating the C-face of SiC, starting with the dome structure formed above. Si atoms did not evaporate from the surface for several hundred ps even at 2000–3000 K. Since nobody knows how Si atoms leave and this process may take a long time, we decided to remove Si atoms in the top layer artificially, all of them together at once ("magic carpet" removal) or individually at

random positions with various periods of removal time. Then, the system was propagated for 12 ps at 2000 K, then a new CSi layer was added to the bottom of the model and the system was propagated for 6 ps before new Si removal process was performed; this cycle was repeated several times. The results for magic carpet removal (those of random removal are similar but less systematic) are shown in Fig. 4B. We observed that some initial surface carbon atoms are lost as C_2 units, since they suddenly lost their Si bond partners. However, most unfilled valences of the two freshly cleaved surface atoms quickly combine into new bonds connecting both layers during the subsequent continued heating at 2000 K, in part facilitating short polyyne chains that are common during QM/MD simulations of high-energy forms of carbon, and which are also found experimentally in high-energy-conditions derived carbon structures. The "arms of the octopus-on-the-rock" clusters that we had observed during fullerene self-assembly are here "tied down" to the surface, effectively preventing closure of a cage structure, and enabling continued tube sidewall growth in perpendicular direction to the surface. The cap re-attachment process actually occurs very fast; after 0.36 ps of the "magic carpet" removal, half of the cap border atoms are already connected to the freshly exposed C surface underneath. Since the cap region does not immediately attach to the SiC surface, the nanocap superstructure becomes visibly "loose" at its dangling side and starts to lose curvature due to the tendency of the π-conjugated sheet towards planarity.

In this structure, we find that the majority of C–Si bonds connecting the CNT to the Si layer are of zigzag type as in the initial structure. The tubes "grown" in our simulations display many sidewall defects, consistent with experimental findings. During random removal of Si on the C-face, we also observe first indications for growth of a second inner tube, as well as buildup of amorphous carbon around the tube/surface interface.

The QM/MD simulation provide insights to the mechanism of fullerene formation and nanotube growth, which is very difficult to clarify experimentally. Growth of carbon nanotubes on the transition-metal cluster is the next target of our QM/MD study.

4. Homogeneous Catalyses and Reactions of Transition-Metal Complexes

We started working on the mechanism of homogeneous catalytic reactions by calculating structures and energies of transition states and intermediates of many elementary steps a little over twenty five years ago. At that time, we encountered a substantial resistance by experimentalists saying that such information is not important in understanding complicated catalytic processes. In the last decades or so theoretical studies of catalytic processes have gained substantial acceptance by experimentalists and proliferation, making it harder to find a paper without theoretical/computational consideration. Reaction pathways of many elementary reactions including oxidative addition, reductive elimination, olefin insertion, metathesis, and bond activation, are now well understood theoretically.[17] However there are several challenges in this field, which we will discuss using our examples.

4.1 Activation of Nitrogen Molecule by Zr Complexes—Subtle Effects of Ligands. One of the present challenges of theoretical studies in homogenous catalysis are adoption of realistic models. In order to tackle intricate effects of different ligands on the mechanism and chemo- and stereo-selectivities, one has to adopt real or realistic models. Nowadays systems containing around hundred or more atoms can be treated by density functional methods or hybrid methods such as ONIOM and OM/MM, allowing to include real ligands as well as some solvent molecules or counter ions, if needed, in the model.

As an example of the effects of subtle difference in the structure of catalyst, here we discuss the activation of nitrogen molecule by metallocence complexes. The activation of molecular nitrogen has been a very active field of research both experimentally and theoretically.[18] Recent experimental studies[19] have shown that zirconocene with four methyl groups on each cyclopentadienyl (C_5Me_4H) activates N_2 molecule to react with three hydrogen molecules under mild condition, while zirconocene with pentamethylcyclopentadienyl (C_5Me_5) cannot make N_2 react with any H_2. These zirconocenes at first form a dimeric N_2 complex, $(Cp_2Zr)(N_2)(ZrCp_2)$, where $Cp = C_5Me_4H$ and C_5Me_5. Our (Bobadova-Parvanova, Musaev, et al.)[20] theoretical calculations have showed that there are two forms of dimeric N_2 complexes, end-on and side-on. The side-on complexes with strong interactions of metal d orbitals with two sets of N_2 π orbitals activate the N_2 molecule to have a long NN distance, so that hydrogen molecule can react easily with this activated N_2. It tuned out among the side-on complexes there is virtually no difference between $Cp = C_5Me_4H$ and C_5Me_5 in the activation energy for the reaction of H_2 molecule. On the other hand, the end-on N_2 complex has rather weak metal–N_2 interaction and the unactivated N_2 in this complex cannot react with any H_2 molecule. As shown in Fig. 5, the most stable form of the dimeric N_2 complex for $Cp = C_5Me_4H$ is a side-on type which reacts H_2 easily. On the other hand, for $Cp = C_5Me_5$ because of steric repulsion between methyl groups on different Zr centers, the side-on complex becomes less stable, and the end-on complex is the most stable form and does not react with any H_2 molecule.

Another intriguing question is why the present zirconocene N_2 complex (called Chirik complex) reacts with three H_2 molecules, while another complex, zirconium diimine N_2 complex, (called Fryzuk complex, see Fig. 6)[18] reacts with only one H_2 molecule under mild condition. Our calculated potential energy profiles for the reaction of the first two H_2 molecules for both complexes are shown in Fig. 6. The barrier for the first H_2 reaction at the TS **1_A3** is about the same for both complexes, both of them should react easily. However, there is a large difference between the two complexes for the second H_2 reaction. For the Chirik complex, the most stable form of the H_2-adduct (**A3**) has one H atom on N and the other on Zr. Addition of the second H_2 molecule to this complex takes place with a reasonable barrier at TS **A5_2**. On the other hand, although the nascent form of the adduct for the Fryzuk complex is also **A3**, this complex bends the Z–N_2–Zr angle and moves the hydrogen atom originally on Zr to the bridge position between two Zr's (**A7**). This is about 10 kcal mol^{-1} more stable than **A3** forming a trap. The second H_2 addition

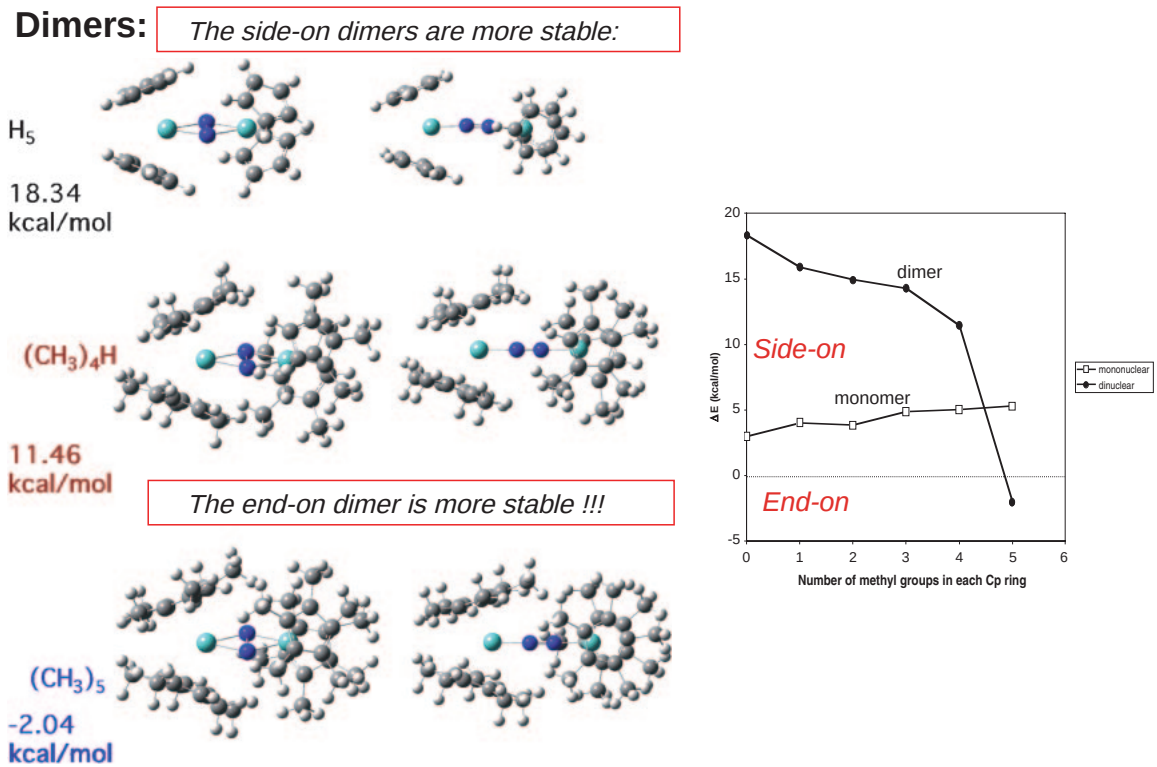

Fig. 5. Two forms of dimeric complex, $(Cp_2Zr)(N_2)(ZrCp_2)$, where $Cp = C_5H_5$, C_5Me_4H, and C_5Me_5. For $Cp = C_5H_5$ and C_5Me_4H, the side-on complex is more stable and can react with H_2. For $Cp = C_5Me_5$, the steric repulsion makes the side-on complex less stable, and the more stable end-on complex cannot react with H_2.

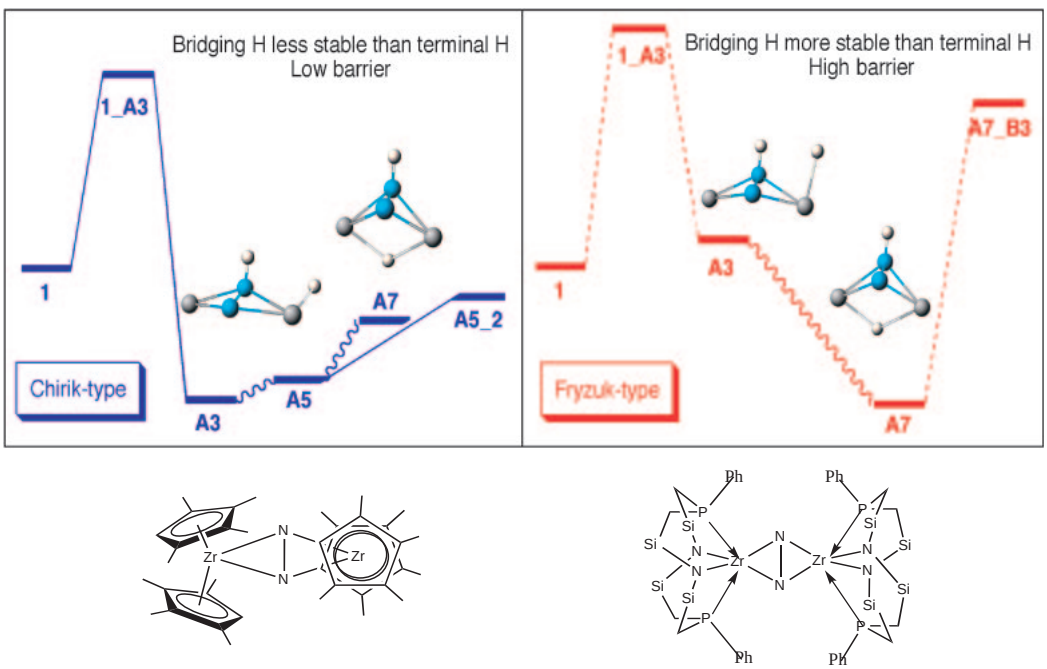

Fig. 6. Comparison of potential energy profile for the activation of the first two hydrogen molecules by Chirik and Fryzuk complexes (Adapted from Bobadova-Parvanova et al., Ref. 20c. Reprinted with permission. Copyright 2006 American Chemical Society.).

from **A7** has a very high barrier at **A7_B3** and cannot take place. The Fryzuk ligand is too flexible, allowing the formation of a stable trapping intermediate. These theoretical calculations have provided insights and guiding principles into intricate effects of substituents and ligands that would not be available easily from experimental studies.

4.2 Olefin Epoxidation by Salen Complex—Contribution of Different Spin States. The second challenge in homo-

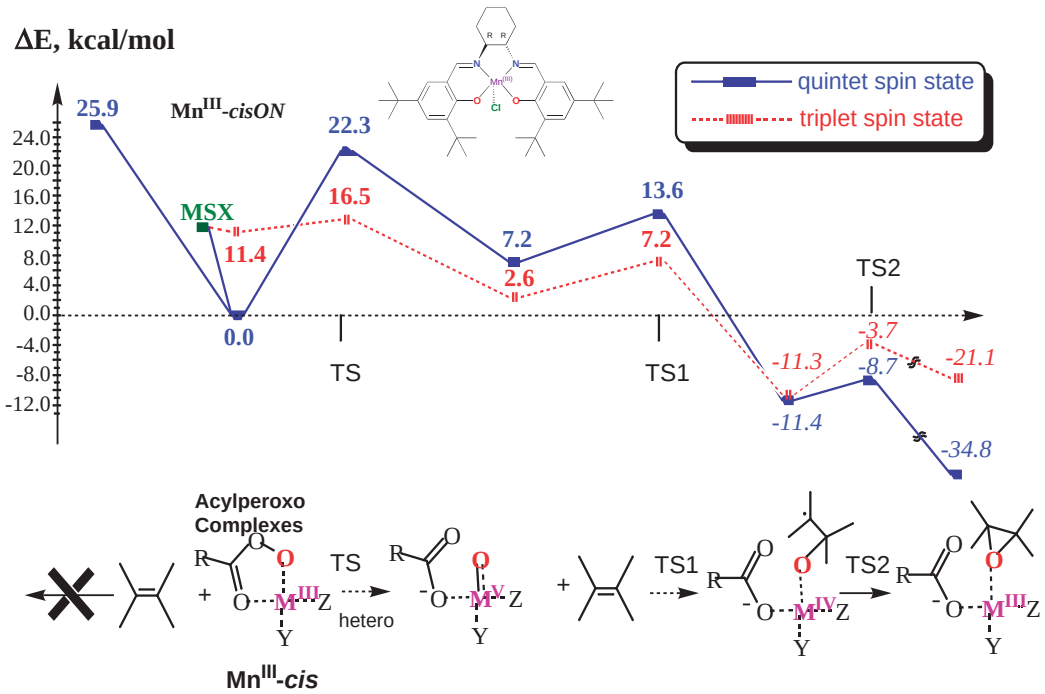

Fig. 7. The potential energy profile of stepwise pathway of the reaction of Mn^{III}-cis form of acylperoxo complex of Salen with olefin to give an epoxide. The lowest path starts with the quintet, crosses over to a triplet state at MSX, and proceeds through the triplet state until a biradical intermediate is formed. Then, the final step takes place in the quintet state.

genous catalysis is explicit consideration of different spin states in the catalysts. Transition-metal complexes, in particular those of first raw transition metals, can easily take different spin states as well as different oxidation states. It has become clearer recently that some catalytic reactions may cascade through different spin states during the course of the reaction. This is sometimes called two-state reaction.[21] The energy minimum on the seam of crossing (MSX) between the potential energy surfaces of different spin states can be considered as the "transition state" for the spin-crossing reaction and can be optimized via energy gradient method.[22] A major problem in the DFT approach is that the relative energies of different spin states depend very sensitively to the amount of the "exact" exchange included in the most commonly used hybrid density function approaches, and the preferred amount of exchange varies case by case. Reliability of a particular hybrid functional for a particular series of compounds has to be tested against experiment or a more reliable theoretical approach, such as coupled-cluster method.[23]

There are now many documented cases of such multi-state reactions. Here, we show as an example the potential energy profile of stepwise pathway of olefin epoxidation by Mn^{III}–Salen acylperoxo complex, from our (Khavrutskii, Musaev, et al.)[24] extensive studies of reactive species and reaction mechanisms of olefin epoxidation and oxidation reactions by Salen complexes. The ground state of Mn^{III}–Salen acylperoxo complex (Y = O, Z = N from Salen), as shown in Fig. 7, was found to be a quintet state. This complex does not react directly with olefin but is at first converted to Mn^{V}–oxo acyl complex. The TS for this conversion in the quintet state is high in energy. However, the TS in the triplet state lies substantially lower in energy than the quintet. An MSX for spin flip has been located not far from the structure of the acylperoxo complex with rather low energy. Thus, the most likely pathway for the reaction is to cross-over from quintet to triplet in the vicinity of the acylperoxo complex, and then follow the triplet pathway through the conversion TS, react with olefin in the triplet through TS1 to produce a biradical intermediate, where triplet and quintet has the same energy, and release epoxide to regenerate Mn^{III} quintet complex.

4.3 Cooperative Effects of Multiple Metal Centers. The third challenges are cooperative effects of multiple metal centers, as often found in multi-metal or cluster complexes. There are reactions that take place only on multiple metal centers as a result of metal cooperative effects. Here, I show our (Khoroshun, Musaev, et al.)[25] little old but still benchmark study of reaction of a tri-ruthenium complex, $(Cp^*)_3Ru_3H_5$ with cyclopentadiene (C_5H_6) leading to formation of the trinuclear 2-methylruthenacyclopentadien, although the reaction itself may not have major catalytic significance. As shown in Fig. 8, this complex **A1** reacts with cyclopentadiene and forms an intermediate **A13**, which converts to the product **B8**. Many possible concerted and stepwise reaction pathways have been followed theoretically, some of which looking promising at an early stage of reaction ended up at the dead end with a high barrier in a following step. At the end the best reaction pathways obtained are shown in Fig. 8. In these pathways, the pentahydrido reactant **A1** loses a hydrogen molecule and coordinates cyclopentadiene either via a dissociative or an associative pathway to generate a trihydrido cyclopentadiene complex **A12**. One of the Ru atoms in this complex then inserts into a cyclopentadiene $C(sp^2)$–$C(sp^3)$ bond to form the experimentally observed intermediate **A13**, which in turn goes through a series of C–H bond formation and cleavage and leads to the

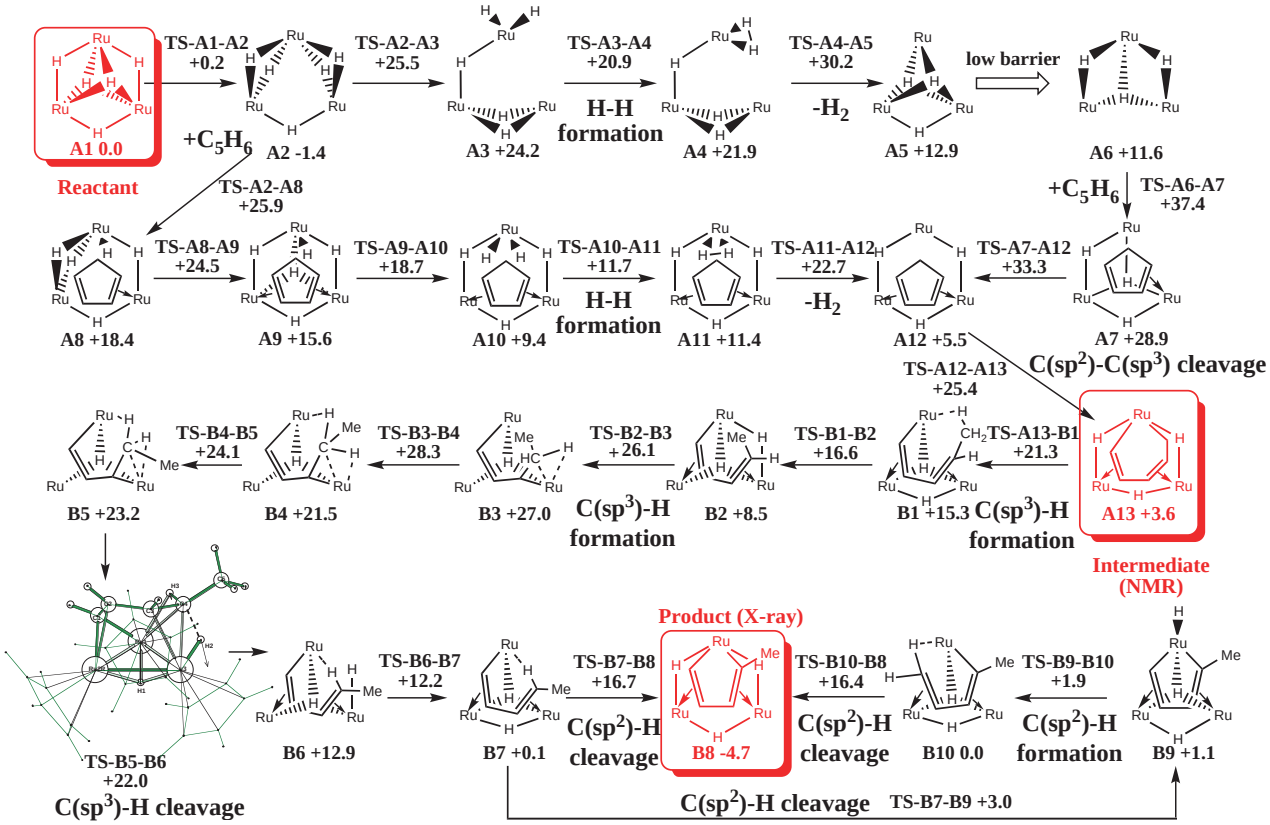

Fig. 8. Most probable reactions pathways for the reaction of $(Cp^*)_3Ru_3H_5$ (**A1**) with cyclopentadiene to leads to **A13** and **B8**. The Gibbs free energies (kcal mol^{-1}, 298 K, 1 atm) of intermediates and transition states are given (Adapted from Khoroshun et al., Ref. 25. Reprinted with permission. Copyright 2003 American Chemical Society.).

experimental final product **B8**. The calculated rate-determining barrier is in good agreement with experiment. An intriguing finding is that the reaction proceeds through many steps, each of which performs one simple task of H transfer among tri-bridged, bridged and terminal positions, pseudorotation around a metal center, coordination and bond formation and breaking. Detailed examination of the structures of intermediates and transition states reveals fascinating collaboration of three metal centers in almost every step of reaction. For instance, the structure of **TS–B5–B6** in Fig. 8 shows that while the reaction coordinate is the transfer of one H atom from C4 to Ru3, Ru2 holds the C4H3 bond to keep the C4H2 bond to the direction of Ru3, and Ru1 interacts with C1–C2 double bond to anchor the substrate at the proper position; a synergetic effort of the three metals to accomplish the goal efficiently. More and more examples are emerging concerning cooperative effects of multiple metal centers, and theoretical studies can provide insight into the electronic origin of such effects.

In this section we showed some examples in which computational studies provided very useful information that is not available experimentally; such as why a small difference in substituents makes a large difference in reactivity, what spin states are responsible to reactivity, and an example of origin of cooperativity of multiple metal centers. Computational/theoretical results have already been used in many patents of homogenous catalysts. I feel that the collaboration between theory and experiment will remain or become more important in the future of catalysis studies.

5. Structure and Reactions of Metalloenzymes and Effects of Protein Environment

Understanding of the mechanism of enzymatic reaction, chemical reaction inside protein, is the largest challenge of theoretical/computational studies of mechanisms of chemical reactions, although this has become a very active field of research last decades or so. Enzyme is a large complex collection of amino acid residues with some metals, ligands and water and other molecules, and theoretical approaches require a substantial approximation. We may consider such studies in three different levels of approaches.[26]

i). Active site only model. In this approach one considers only atoms of the active site (including real or model ligands in the first coordination shell around the central metals or other active centers), substrates and water molecules directly involved in the reaction. Nowadays active site models typically contain around 100 atoms. The structures of reactants, intermediates, and transition states of this model reaction system are optimized with an appropriate QM method (nowadays mostly at a DFT level), activation barriers are evaluated and the reaction mechanisms are discussed. The active site only approach should work better for metalloenzymes where reactions tend to occur localized in the vicinity of metals than for non-metal enzymes where reactions may be take place delocalized in a wider area. In this approach, any explicit effects of protein environment are completely neglected or are approximated by a homogenous dielectric medium.

ii). Protein model with geometry optimization. Here, typically starting with an X-ray structure of the protein (including some water molecules), a model is designed by selecting atoms within a certain range from the metal centers (mending dangling bonds in the protein backbones by appropriate groups). Then, one adds hydrogen atoms and substrates, if not included in X-ray structure, to construct a model typically containing thousands of atoms. Geometry optimization (full or typically under certain constraints) is performed for complexes, intermediates and transition states and calculate barriers. Since the conformational space of the protein is very extensive, care must be taken so that changes in protein structure are directly coupled to the reaction coordinate, and not to arbitrary conformational changes during the optimization. A conservative solution is to use similar structures for reactant and product, but even this is technically very difficult to achieve and often requires improved optimization algorithms[27] to stay in the same local MM minima during a reaction step. Since it is impossible to perform QM calculations for such a large system, a hybrid method, such as QM/MM and ONIOM method, is adopted, in which the system is divided in parts where a more accurate method (e.g., DFT) is used where the reaction actually takes place and less accurate methods (e.g. semi-empirical QM or MM) are used for less important regions of the system. Comparison of the results of the protein model with those of the active-site model reveals the role of protein environment in the reaction.

iii). Statistical average of protein motion/conformations and free energy calculation. In order to sample a large conformational space of protein, it is desirable to take statistical average of conformational space and obtain a "free energy" reaction profile. The most popular method used in protein models, DFT/MM, is still very expensive for statistical averaging and there are only very few free energy calculations published at this level. However, different efforts have been made, including statistical averaging at a lower level (say pure MM or semi-empirical QM/MM) combined with DFT/MM calculations. Accurate description of statistics and dynamics of reactions of large molecular systems like enzymes is a major challenge at present and I expect great activities in this area for the coming decade.

In this section, we concentrate on the approach ii) above and discuss some examples we have studied with the protein model (using ONIOM DFT:MM) as well as the active site model (DFT) with geometry optimization.

5.1 Isopenicillin N-Synthase—Substantial Effects of Protein Environment on Energetics. The first example (Lundberg, et al.)[28] is the conversion of the linear tripeptide substrate δ-(L-α-aminoadipoyl)-L-cysteinyl-D-valine (ACV) to isopenicillin N by the use of a molecular oxygen catalyzed by isopenicillin N-synthase (IPNS), a non-heme iron enzyme.[29] Here, the real system we adopted contains 5386 atoms, while the active site model or the QM part consists of 65 atoms (or less in later stages when some products were removed). Figure 9 shows the potential energy profiles of the entire catalytic process following the proposed mechanism consisting of several steps of reactions. The potential profile using the active site model is qualitatively similar to that with the protein model obtained with the ONIOM(DFT:MM) method, with an average difference of barriers of ca. 3 kcal mol^{-1}. However, the largest difference is 10 kcal mol^{-1} in the rate-determining first activation step. This difference makes the reaction easy to occur from difficult to occur in room temperature, a typical role of a catalyst in catalytic reaction. Related to this is the observation that coordination of molecular oxygen at the beginning of the catalytic cycle becomes from endothermic to thermoneutral in the presence of protein environment. Detailed analysis of QM part and various MM energy components clarifies the origin of energy changes, as commented directly in Fig. 9. This analysis indicates that the van der Waals interaction between the oxygen molecule and near-by protein residues, neglected in the active-site-only model, favors oxygen binding.

5.2 Glutathione Peroxidases—Small Protein Environment Effect on Energetics. Glutathione peroxidases (GPx) are a family of selenoproteins, which show a strong anti-oxidant activity and protect cells against oxidative damage.[30] These enzymes use glutathione to reduce reactive oxygen species like hydrogen peroxide and organic peroxides. We (Prabhakar, Musaev, et al.)[31] have carried out extensive computational studies on the structure and reactivities of GPx with both the active site DFT model (86 atoms) and the protein ONIOM DFT:MM model (with the entire monomer of GPx of 3113 atoms plus two water molecules), as shown in Figs. 10B and 10A, respectively. For this system a comparison of the active site structure from the ONIOM optimized structure and that from the X-ray structure, which usually agree well, showed unusual RMS errors. Calculations performed with two additional water molecules at the active site reduced the RMS deviation and suggested the presence of water molecules (missed in the X-ray structure) in the active site of GPx. These water molecules turned out to be important and participate in the enzymatic reaction.

The total catalytic reaction in GPx can be divided into three steps. The first reaction of the catalytic process, (E-SeH) + H_2O_2 → (E-SeOH) + H_2O, proceeds via a stepwise pathway with an overall barrier of 17.1 kcal mol^{-1}, in good agreement with the experimental barrier of 14.9 kcal mol^{-1}. During the reaction, Gln83 residue plays a key role as a proton acceptor, also consistent with experiments. The second step, (E-SeOH) + GSH → (E-Se-SG) + H_2O, proceeds with a barrier of 17.9 kcal mol^{-1}. The third step, (E-Se-SG) + GSH → (E-SeH) + GS-SG, is initiated by the coordination of the second glutathione molecule. The calculations suggest that the amide backbone of Gly50 residue directly participates in this reaction. The two water molecules are absolutely vital because they act as proton shuttles between the second glutathione molecule and the selenocysteine residue. This reaction proceeds with the barrier of 21.5 kcal mol^{-1}, and is suggested to be a rate-determining step of the entire GPx catalyzed reaction. For the present reaction, the effect of surrounding protein on the potential energy profile is small, as illustrated in Fig. 10C for the first reaction step. A possible reason for the small protein effects could be that in this enzyme the active site is located on the interface of two monomer, rather than deeply buried inside the protein. We also noted that the protein environment had substantial effects on the active-site geometry. The reason this does not affect the total

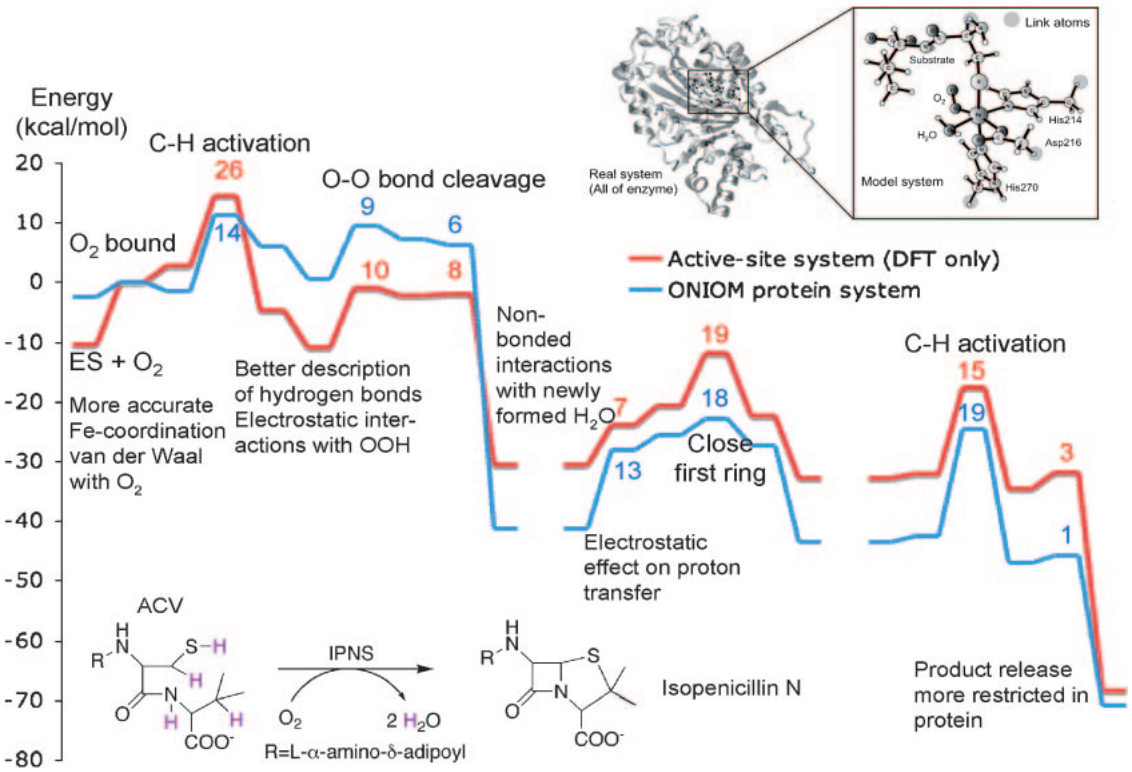

Fig. 9. Potential energy profiles of oxidation of ACV substrate to form isopenicillin N catalyzed by IPNS, using the active site model (DFT, red) and the protein model (DTF/MM, blue).

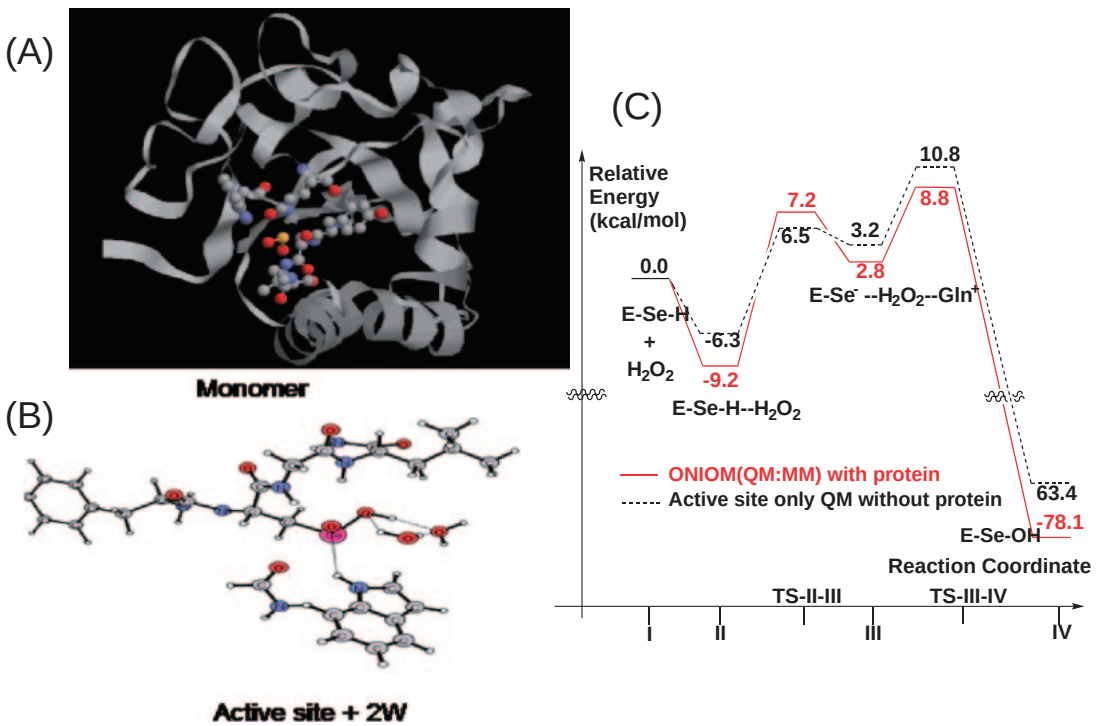

Fig. 10. (A) The real system, the entire monomer unit of GPX. (B) Active site with two water molecules added. (C) Potential energy profile of the fist stage of reaction: (E–SeH) + H_2O_2 → (E–SeOH) + H_2O, with the active site only QM calculation and the ONIOM calculation with protein (Adapted from Prabhakar et al., Refs. 31c and 31d. Reprinted with permission. Copyright 2005, 2006 American Chemical Society.).

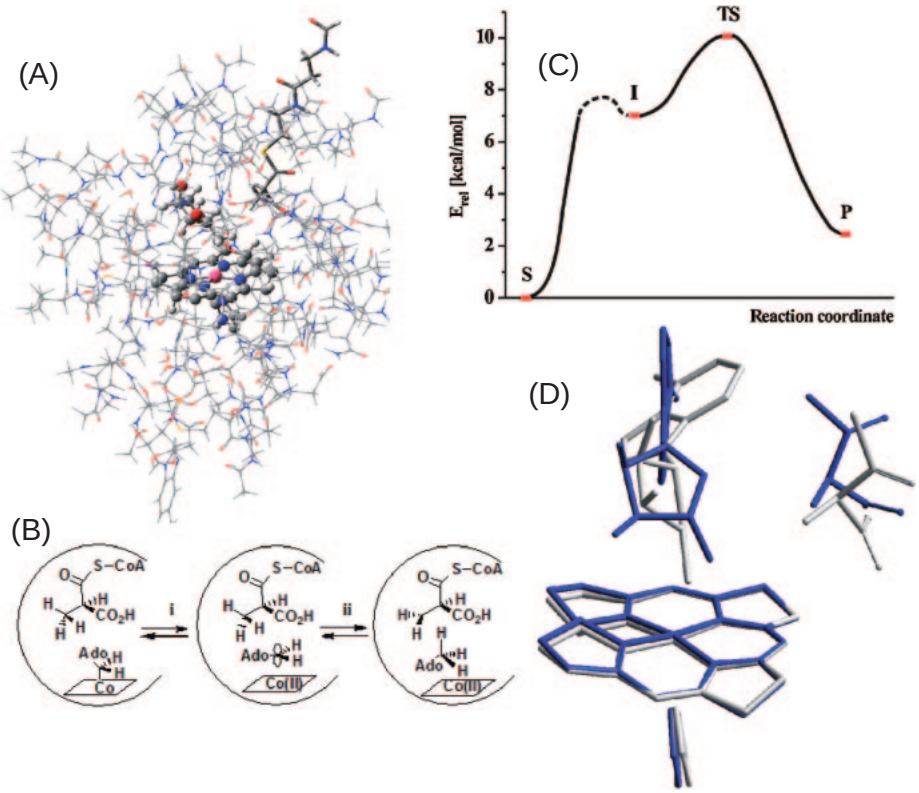

Fig. 11. (A) QM (ball-and-stick) and MM part of the model of MCM. (B) The step i of this reaction is studied here. (C) The potential energy profile in the protein. (D) The superposition of the active site conformations at the initial structure (S in (C), grey) and the transition structure (TS, blue) (Adapted from Kwiecien et al., Ref. 33. Reprinted with permission. Copyright 2006 American Chemical Society.).

barrier height is that when comparing transition state and reactant, the protein effect appears to be relatively similar and does not change activation energy.

5.3 Methylmalonyl-CoA Mutase—Positive Participation of Protein Environments in Reaction Coordinate. Methylmalonyl-CoA mutase (MCM) catalyzes a radical-based transformation of methylmalonyl-CoA (MCA) to succinyl-CoA.[32] The cofactor adenosylcobalamin (AdoCbl) serves as a radical reservoir that generates the 5′-deoxyadenosine radical (dAdo•) via homolysis of the Co–C5′ bond (Fig. 11B). The mechanism by which the enzyme stabilizes the homolysis products and achieve an observed $\approx 10^{12}$-fold rate acceleration is not yet fully understood. Co–C bond homolysis is directly kinetically coupled to the proceeding hydrogen atom transfer step and the products of the bond homolysis step have therefore not been experimentally characterized. Recently, we (Kwiecien et al.)[33] performed an ONIOM QM:MM study to reveal the role of the protein in the rupture of the Co–C5′ bond. The ONIOM protein system contains the substrate, methylmalonyl-CoA, bound to the active site, the cofactor (AdoCbl) and all amino acids within a 15-Å radius from the cobalt atom, and the active-site (QM part) contains a truncated AdoCbl and the imidazole ring of its lower ligand, as shown in Fig. 11A. The potential energy profile for the Co–C5′ bond homolysis obtained in the ONIOM calculation is shown in Fig. 11C. The comparison of optimized structures of initial enzyme (**R**), intermediate (**I**), and transition state (**TS**) (see Fig. 11D) indicates that a dramatic change in the conformational features of the dAdo moiety has taken place between **R** and **I**. This conformational change caused slight Co–C5′ bond elongation, which is connected to a destabilization of the AdoCbl. The subsequent homolysis from **I** is characterized by a very small energy barrier of ≈ 3 kcal mol^{-1} and is exothermic by ≈ 7.5 kcal mol^{-1}. Thus in the case of MCM, change in the protein environment around the active site is a part of the reaction coordinate, and it is essential to include this protein environment for calculating the energy profile of cobalt–carbon bond homolysis.

Although we do not have many examples yet, our ONIOM studies on the effects of protein environments in metalloenzymatic reactions have revealed some different situations. Typically, we found that the protein environment does not change the reaction pathway or mechanism of metalloenzymatic reactions but does change the energetics and therefore the rate of reaction, a typical role of a catalyst. We also saw a case where the effect of protein on energetics is small, when the active site is on the surface of protein or when the protein effects on the transition state is comparable to that on the reactant. We also saw a case in which the protein environment is an active participant in the reaction, where the active site only model will totally fail in describing the reaction pathway or reaction coordinate.

The task is just started to learn more about the reaction of enzymes from computational studies. More realistic models, more reliable calculations, more statistical averaging, and long time dynamics—with all these, on some day we hope to understand enzymatic reactions much better than we do now.

6. Perspective

The theoretical/computational study of chemical reactions has been and still is a very exciting field of chemistry. It provides insight into the detailed mechanism, pathways, energetics, dynamics of complex reactions mechanism, the information that is not easily available from experiments and complementary to experiments. Although quantum chemistry that gives the optimized structures and energies of reactants, intermediates and transition states plays the key role in this respect, in some cases molecule dynamics is essential to represent many possible pathways of reactions. Multiple potential energy surfaces arising from many electronic and spin states and transition among them are key players in reactions of excited states (photochemistry) and some transition-metal complexes. Subtle differences in substituent effects in organic and organometallic chemistry make reactions chemo-, regio-, and stereo-selective, and the control of such differences by theoretical calculations is a very important issue that will require a lot of attention. Understanding and hopefully controlling enzymatic reactions is the ultimate goal of theoretical studies of complex molecular systems, which I would say has just began a long and difficult journey.

For accurate long time simulation of complex molecular systems, the present computing power is insufficient. For instance it is not easy to run DFT/MM dynamics for ns for an enzymatic reactions. Arrival of faster computers, including "next-generation supercomputer" of 10 peta flop speed scheduled to be in operation in 2011,[34] is anxiously waited for. Such new computers will make it possible to carry out such demanding calculations and will give a great opportunity to theoretical/computational chemistry to make a profound impact in the progress of chemical research.

In the coming decade or so, understanding chemical reactions of complex molecular systems will remain to be the central issue of theoretical/computational chemistry. In order to accomplish this goal, we have to use all the theoretical/computational methodologies available to us: quantum chemistry, classical and quantum molecular dynamics, long time simulation and statistical averaging. After fifty years of my career, I find this field still very fascinating and believe that it will remain exciting for the foreseeable future. I hope that younger generations also find this field very exciting and take leadership in promoting this endeavor.

Acknowledgement is made to all my students, postdocs, collaborators, and sponsors for making possible this exciting venture into the world of chemical reactions. Particular thanks go to Ioannis Kerkines, Zhi Wang, Peng Zhang, Stephan Irle, Guishan Zheng, Petia Bobadova-Parvanova, Jamal Musaev, Ilja Khavrutskii, Dima Khoroshun, Marcus Lundberg, Rajeev Prabhakar, Renata Kwiecien, and Piotr Paneth, whose studies are discussed in this article. The work at Kyoto University is supported in part by the Fukui Institute for Fundamental Chemistry and in part by a CREST (Core Research for Evolutional Science and Technology) grant in the area of High Performance Computing for Multi-Scale and Multi-Physics Phenomena from of JST (Japan Science and Technology Agency). The work at Emory is in part supported by US Air Force Office of Scientific Research.

References

1 A. Warshel, M. Levitt, *J. Mol. Biol.* **1976**, *103*, 227.

2 a) F. Maseras, K. Morokuma, *J. Comput. Chem.* **1995**, *16*, 1170. b) M. Svensson, S. Humbel, R. D. J. Froese, T. Matsubara, S. Sieber, K. Morokuma, *J. Phys. Chem.* **1996**, *100*, 19357. c) S. Dapprich, I. Komaromi, K. S. Byun, K. Morokuma, M. J. Frisch, *THEOCHEM* **1999**, *461–462*, 1. d) T. Vreven, K. Morokuma, *J. Comput. Chem.* **2000**, *21*, 1419. e) K. Morokuma, *Bull. Korean Chem. Soc.* **2003**, *24*, 797. f) T. Vreven, K. Morokuma, *Ann. Rep. Comput. Chem.* **2006**, *2*, 35. g) T. Vreven, K. S. Byun, I. Komáromi, S. Dapprich, J. A. Montgomery, Jr., K. Morokuma, M. J. Frisch, *J. Chem. Theory Comput.* **2006**, *2*, 815.

3 A few recent examples: a) A. J. Midey, A. I. Fernandez, A. A. Viggiano, P. Zhang, K. Morokuma, *J. Chem. Phys.* **2006**, *124*, 114313. b) J. Zhang, P. Zhang, Y. Chen, K. Yuan, S. A. Harich, X. Wang, Z. Wang, X. Yang, K. Morokuma, A. M. Wodtke, *Phys. Chem. Chem. Phys.* **2006**, *8*, 1690. c) P. Zhang, G. S. Tschumper, S. Irle, K. Morokuma, *J. Chem. Phys.* **2003**, *119*, 6524.

4 a) N. Hansen, A. M. Wodtke, *J. Phys. Chem. A* **2003**, *107*, 10608. b) S. J. Goncher, N. E. Sveum, D. T. Moore, N. D. Bartlett, D. M. Neumark, *J. Chem. Phys.* **2006**, *125*, 224304. c) P. C. Samartzis, J. J.-M. Lin, T.-T. Ching, C. Chaudhuri, S.-H. Lee, A. M. Wodtke, *J. Chem. Phys.* **2007**, *126*, 041101.

5 I. S. K. Kerkines, Z. Wang, P. Zhang, K. Morokuma, *J. Chem. Phys.*, to be published.

6 J. Maul, Th. Berg, E. Marosits, G. Schonhense, G. Huber, *Phys. Rev. B* **2006**, *74*, 161406.

7 For a review, see for instance: T. Yamaguchi, S. Maruyama, *JSME Int. J., Ser. B* **1997**, *63*, 2398.

8 a) G. Nicolis, I. Prigogine, *Self-Organization in Nonequilibrium Systems: From Dissipative Structures to Order through Fluctuations*, Wiley, New York, **1977**. b) I. Prigogine, *The End of Certainty—Time, Chaos, and the New Laws of Nature*, The Free Press, New York, **1997**.

9 a) D. W. Brenner, *Phys. Rev. B* **1990**, *42*, 9458. b) D. W. Brenner, J. A. Harrison, C. T. White, R. J. Colton, *Thin Solid Films* **1991**, *206*, 220. c) D. W. Brenner, O. A. Shenderova, J. A. Harrison, S. J. Stuart, B. Ni, S. B. Sinnott, *J. Phys.: Condens. Matter* **2002**, *14*, 783.

10 a) D. Porezag, T. Frauenheim, T. Köhler, G. Seifert, R. Kaschner, *Phys. Rev. B* **1995**, *51*, 12947. b) M. Elstner, D. Porezag, G. Jungnickel, J. Elsner, M. Haugk, T. Frauenheim, S. Suhai, G. Seifert, *Phys. Rev. B* **1998**, *58*, 7260.

11 a) Y. Yamaguchi, S. Maruyama, *Chem. Phys. Lett.* **1998**, *286*, 336. b) S. Maruyama, Y. Yamaguchi, *Chem. Phys. Lett.* **1998**, *286*, 343.

12 a) S. Irle, G. Zheng, M. Elstner, K. Morokuma, *Nano Lett.* **2003**, *3*, 465. b) S. Irle, G. Zheng, M. Elstner, K. Morokuma, *Nano Lett.* **2003**, *3*, 1657. c) G. Zheng, S. Irle, M. Elstner, K. Morokuma, *J. Phys. Chem. A* **2004**, *108*, 3182. d) G. Zheng, S. Irle, M. Elstner, K. Morokuma, *J. Chem. Phys.* **2005**, *122*, 014708. e) S. Irle, G. Zheng, Z. Wang, K. Morokuma, *J. Phys. Chem. B* **2006**, *110*, 14531. f) G. Zheng, Z. Wang, S. Irle, K. Morokuma, *J. Nanosci. Nanotechnol.* **2007**, *7*, 1662. g) S. Irle, G. Zheng, Z. Wang, K. Morokuma, *Nano* **2007**, *2*, 21. h) Z. Wang, S. Irle, K. Morokuma, unpublished.

13 S. Irle, B. Finck, K. Morokuma, to be published.

14 a) S. Iijima, T. Ishihashi, *Nature* **1993**, *363*, 603. b) D. S. Bethune, C. Kiang, M. S. DeVries, G. Gorman, R. Savoy, R. Beyers, *Nature* **1993**, *363*, 605. c) A. Thess, R. Lee, P. Nikolaev,

H. J. Dai, P. Petit, J. Robert, C. H. Xu, Y. H. Lee, S. G. Kim, A. G. Rinzler, D. T. Colbert, G. E. Scuseria, D. Tomanek, J. E. Fischer, R. E. Smalley, *Science* **1996**, *273*, 483.

15 a) M. Kusunoki, T. Suzuki, K. Kaneko, M. Ito, *Philos. Mag. Lett.* **1999**, *79*, 153. b) M. Kusunoki, T. Suzuki, T. Hirayama, N. Shibata, K. Kaneko, *Appl. Phys. Lett.* **2000**, *77*, 531. c) M. Kusunoki, T. Suzuki, C. Honjo, T. Hirayama, N. Shibata, *Chem. Phys. Lett.* **2002**, *366*, 458. d) M. Kusunoki, C. Honjo, T. Suzuki, T. Hirayama, *Appl. Phys. Lett.* **2005**, *87*, 103105. e) V. Derycke, R. Martel, M. Radosvljevic, F. M. R. Ross, P. Avouris, *Nano Lett.* **2002**, *2*, 1043.

16 a) S. Irle, Z. Wang, G. Zheng, K. Morokuma, M. Kusunoki, *J. Chem. Phys.* **2006**, *125*, 044702. b) Z. Wang, S. Irle, G. Zheng, M. Kusunoki, K. Morokuma, *J. Phys. Chem. C* **2007**, *111*, 12960.

17 For reviews, for instance: *Computational Modeling of Principles and Mechanisms of Transition Metal-Based Homogenous Catalytic Processes*, ed. by K. Morokuma, D. G. Musaev, Wiley-VCH, **2007**.

18 a) M. D. Fryzuk, S. A. Johnson, *Coord. Chem. Rev.* **2000**, *200–202*, 379. b) J. R. in *Catalytic Ammonia Synthesis*, ed. by Jennings, Plenum, New York, **1991**. c) M. D. Fryzuk, *Nature* **2004**, *427*, 498. d) R. Schlögl, *Angew. Chem., Int. Ed.* **2003**, *42*, 2004. e) M. Mori, *J. Organomet. Chem.* **2004**, *689*, 4210. f) D. V. Yandulov, R. R. Schrock, *Science* **2003**, *301*, 76. g) R. R. Schrock, *Acc. Chem. Res.* **2005**, *38*, 955. h) B. A. MacKay, M. D. Fryzuk, *Chem. Rev.* **2004**, *104*, 385. i) S. Gambarotta, J. Scott, *Angew. Chem., Int. Ed.* **2004**, *43*, 5298.

19 a) J. A. Pool, E. Lobkovsky, P. J. Chirik, *Nature* **2004**, *427*, 527. b) W. H. Bernskoetter, E. Lobkovsky, P. J. Chirik, *J. Am. Chem. Soc.* **2005**, *127*, 14051.

20 a) P. Bobadova-Parvanova, Q. Wang, K. Morokuma, D. G. Musaev, *Angew. Chem., Int. Ed.* **2005**, *44*, 7101. b) P. Bobadova-Parvanova, D. Quinonero, K. Morokuma, D. G. Musaev, *J. Chem. Theory Comput.* **2006**, *2*, 336. c) P. Bobadova-Parvanova, Q. Wang, D. Quinonero, K. Morokuma, D. G. Musaev, *J. Am. Chem. Soc.* **2006**, *128*, 11391. d) D. G. Musaev, P. Bobadova-Parvanova, K. Morokuma, *Inorg. Chem.* **2007**, *46*, 2709.

21 For a review: S. Shaik, S. P. de Visser, F. Ogliaro, H. Schwarz, D. Schroder, *Curr. Opin. Chem. Biol.* **2002**, *6*, 556.

22 a) N. Koga, K. Morokuma, *Chem. Phys. Lett.* **1985**, *119*, 371. b) Q. Cui, K. Morokuma, J. F. Stanton, *Chem. Phys. Lett.* **1996**, *263*, 46. c) Q. Cui, K. Morokuma, *Theor. Chem. Acc.* **1999**, *102*, 127.

23 D. Quiñonero, K. Morokuma, D. G. Musaev, R. Mas-Ballesté, L. Que, Jr., *J. Am. Chem. Soc.* **2005**, *127*, 6548.

24 a) I. V. Khavrutskii, D. G. Musaev, K. Morokuma, *Inorg. Chem.* **2003**, *42*, 2606. b) I. V. Khavrutskii, D. G. Musaev, K. Morokuma, *J. Am. Chem. Soc.* **2003**, *125*, 13879. c) I. V. Khavrutskii, R. R. Rahim, D. G. Musaev, K. Morokuma, *J. Phys. Chem. B* **2004**, *108*, 3845. d) I. V. Khavrutskii, D. G. Musaev, K. Morokuma, *Proc. Natl. Acad. Sci. U.S.A.* **2004**, *101*, 5743. e) I. V. Khavrutskii, D. G. Musaev, K. Morokuma, *Inorg. Chem.* **2005**, *44*, 306.

25 D. V. Khoroshun, A. Inagaki, H. Suzuki, S. F. Vyboischikov, D. G. Musaev, K. Morokuma, *J. Am. Chem. Soc.* **2003**, *125*, 9910.

26 M. Lundberg, K. Morokuma, in *Multi-Scale Quantum Models for Biocatalysis: Modern Techniques and Applications*, ed. by T.-S. Lee, D. M. York, Springer Verlag, **2007**.

27 a) T. Vreven, K. Morokuma, Ö. Farkas, H. B. Schlegel, M. J. Frisch, *J. Comput. Chem.* **2003**, *24*, 760. b) T. Vreven, M. J. Frisch, K. N. Kudin, H. B. Schlegel, K. Morokuma, *Mol. Phys.* **2006**, *104*, 701.

28 a) M. Lundberg, K. Morokuma, *J. Phys. Chem. B* **2007**, *111*, 9380. b) M. Lundberg, P. E. M. Siegbahn, K. Morokuma, submitted for publication. c) M. Lundberg, K. Morokuma, to be published.

29 a) P. L. Roach, I. J. Clifton, C. M. H. Hensgens, N. Shibata, C. J. Schofield, J. E. Baldwin, *Nature* **1997**, *387*, 827. b) N. I. Burzlaff, P. J. Rutledge, I. J. Clifton, C. M. H. Hensgens, M. Pickford, R. M. Adlington, P. L. Roach, J. E. Baldwin, *Nature* **1999**, *401*, 721.

30 a) B. Ren, W. Huang, B. Åkesson, R. Ladenstein, *J. Mol. Biol.* **1997**, *268*, 869. b) L. Flohè, in *Glutathione*, ed. by D. Dolphin, O. Avramovic, R. Poulson, John Wiley, New York, **1989**, pp. 644–731.

31 a) R. Prabhakar, D. G. Musaev, I. V. Khavrutskii, K. Morokuma, *J. Phys. Chem. B* **2004**, *108*, 12643. b) R. Prabhakar, D. G. Musaev, I. V. Khavrutskii, K. Morokuma, *J. Phys. Chem. B* **2004**, *108*, 12643. c) R. Prabhakar, K. Morokuma, D. G. Musaev, *Biochemistry* **2006**, *45*, 6967. d) R. Prabhakar, T. Vreven, M. Frisch, K. Morokuma, D. G. Musaev, *J. Phys. Chem. B* **2006**, *110*, 13608.

32 a) F. Mancia, P. R. Evans, *Structure* **1998**, *6*, 711. b) R. Banerjee, *Chem. Rev.* **2003**, *103*, 2081.

33 R. A. Kwiecien, I. V. Khavrutskii, D. G. Musaev, K. Morokuma, R. Banerjee, P. Paneth, *J. Am. Chem. Soc.* **2006**, *128*, 1287.

34 http://www.nsc.riken.jp/project-eng.html.

Since fall 2006 Keiji Morokuma is Research Leader at Fukui Institute for Fundamental Chemistry at Kyoto University and William H. Emerson Professor Emeritus at Emory University. He now spends 100% of time in research (which he enjoys most) and splits time between the two inisitutions. At Kyoto he is the Principal Investigator of a CREST (Core Research for Evolutional Science and Technology) grant from JST in the Area of High Performance Computing for Multi-scale and Multi-physics and leads a group of 8 postdocs, one assistant, and 4 undergraduates. The Emory group consists of 4 postdocs, one graduate student, and one undergraduate. Both groups hold a weekly joint discussion meeting on internet. After finishing his Ph.D. under Prof. Kenichi Fukui at Kyoto University, he was a professor at University of Rochester and Institute for Molecular Science at Okazaki, Japan, before taking up his appointment at Emory in 1993. Prof. Morokuma has authored over 600 scientific publications and received numerous scientific awards, including Japan Chemical Society Award, Schrödinger Medal from World Association of Theoretical Organic Chemists and Fukui Medal of Asian Pacific Association of Theoretical & Computational Chemists. He served as President of International Academy of Quantum Molecular Science for 2000–2006.